



New diterpene furanoids from the Antarctic lichen *Huea* sp

Yinglan Cui^a, Joung Han Yim^b, Dong-Sung Lee^c, Youn-Chul Kim^c, Hyuncheol Oh^{c,*}

^a College of Medical and Life Sciences, Silla University, Busan 617-736, Republic of Korea

^b Korea Polar Research Institute, KORDI, 7-50 Songdo-dong, Yeosu-gu, Incheon 406-840, Republic of Korea

^c College of Pharmacy, Wonkwang University, Iksan 570-749, Republic of Korea

ARTICLE INFO

Article history:

Received 19 July 2012

Revised 12 October 2012

Accepted 15 October 2012

Available online 23 October 2012

Keywords:

Huea sp

Protein tyrosine phosphatase 1B (PTP1B)

Diterpene furanoids

Non-competitive inhibitor

ABSTRACT

In the course of ongoing research on protein tyrosine phosphatase 1B (PTP1B) inhibitory compounds from Antarctic lichens, four new diterpene furanoids, hueafuranoids A–D (**1–4**) have been isolated from the MeOH extract of Antarctic lichen *Huea* sp. by various chromatographic methods. The structures of these compounds were elucidated by analysis of NMR and MS data, and comparing their spectral data with those in the literature. Compound **1** showed inhibitory activity against therapeutically targeted protein, PTP1B with an IC₅₀ value of 13.9 μM. The kinetic analysis of PTP1B inhibition by hueafuranoid A (**1**) suggested that the diterpene furanoids encountered in this study inhibited PTP1B activity in a non-competitive manner.

© 2012 Elsevier Ltd. All rights reserved.

Protein tyrosine phosphatase 1B (PTP1B) is a widely expressed protein tyrosine phosphatase that is present in insulin-sensitive tissues. PTP1B knockout mice have proven to be hypersensitive to insulin and resistant to obesity, but they lack other significant negative side-effects.^{1,2} In addition, PTP1B regulates leptin action, which controls satiety and energy expenditure.³ PTP1B-deficient mice have remarkably low adiposity, and are protected from diet-induced obesity by increases in basal metabolic rate and total energy expenditure. This result is consistent with the inference that PTP1B is a major regulator of energy balance, insulin sensitivity, and body fat stores in vivo.⁴ Thus, inhibition of PTP1B is suggested to be an excellent, novel therapy for targeting type 2 diabetes and obesity.³ Considering the compelling biochemical and genetic evidence that links PTP1B to several human diseases, a number of studies have been performed in the fields of synthetic/medicinal chemistry to develop PTP1B inhibitors.^{5,6} On the other hand, screening for PTP1B inhibitors from natural products, which have an excellent track record of success in small molecule drug discovery programs, has begun only recently compared to the relatively intensive efforts which involve synthetic studies.⁷

Lichens are symbiotic organisms consisting of a fungus that cultivates a photosynthesizing partner that can be either an alga or a cyanobacterium.⁸ In all lichens, the fungus forms a thallus or lichenized stroma that may contain characteristic secondary metabolites, and these metabolites are sometimes suggested to serve as antimicrobial or antiherbivore agents.⁹ Lichens evolved several biosynthetic pathways, mainly the polyketide pathway, to produce

diverse secondary metabolites, and most of these metabolites are produced by the fungus in a symbiosis or an aposymbiotic state. Lichen compounds are often structurally unique, and only a small portion of the known lichen metabolites are found in other fungi or higher plants.¹⁰ In addition, the production of lichen metabolites is sometimes correlated with the lichen morphology and geography in individuals at the species and genus levels.¹¹ Several lichen extracts have been used as various remedies in folk medicine, and a variety of biological activities of lichen metabolites, including antibiotic, antimycobacterial, antiviral, analgesic, antipyretic, and antioxidative properties, have been indicated by screening processes.^{8,11,12} Thus, there is a considerable interest in lichen metabolites, especially those from unexplored lichens, as potential sources of pharmacological agents.

In the course of our ongoing studies for PTP1B inhibitory Antarctic lichen metabolites,^{13–16} the MeOH extract of a dried sample of *Huea* sp. was selected for further study based on the observation of significant PTP1B inhibitory effect at the extract level (>90% inhibition at 30 μg/mL). Bioassay-guided fractionation of the extract led to the isolation of four new lichen metabolites, which belong to the class of diterpenoids, which we named hueafuranoids A–D (**1–4**) (Fig. 1). This report describes the isolation, structure elucidation, and biological activities of the compounds encountered in this study.

A dried sample of *Huea* sp. was extracted with MeOH (9 L) for 24 h. The resulting crude MeOH extract (7.0 g) was subjected to C₁₈-functionalized silica gel flash column chromatography, eluting with a stepwise gradient of 20%, 40%, 60%, 80%, and 100% (v/v) MeOH in H₂O (500 mL each). The fraction eluted with 80% MeOH was re-applied to C₁₈-functionalized silica gel flash column

* Corresponding author. Tel.: +82 63 850 6815; fax: +82 63 852 8837.

E-mail address: hoh@wonkwang.ac.kr (H. Oh).

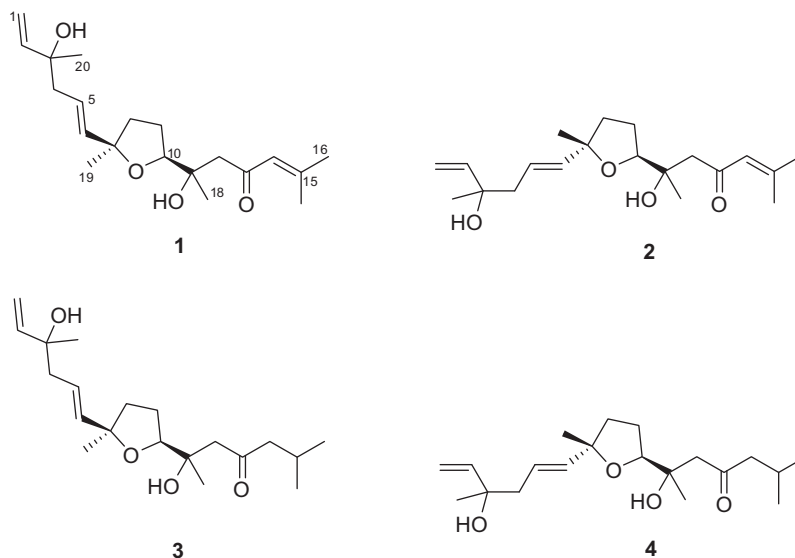


Figure 1. Chemical structures of compounds 1–4.

chromatography, eluting with a stepwise gradient of MeOH in H₂O. The fraction eluted with 70% MeOH in H₂O was then subjected to semi-preparative reversed phase HPLC using a gradient from 20% to 60% CH₃CN in H₂O (0.1% formic acid) over 80 min to yield compounds **1** (1.7 mg; *t_R* = 48 min) and **2** (0.9 mg; *t_R* = 49 min). The fraction eluted with 75% MeOH in H₂O was subjected to semi-preparative reversed phase HPLC using a gradient from 40% to 60% CH₃CN in H₂O over 80 min to yield compounds **3** (0.3 mg; *t_R* = 41 min) and **4** (0.3 mg; *t_R* = 44 min).

Hueafuranoid A (**1**) has the molecular formula C₂₀H₃₂O₄, as deduced from HRESIMS [*m/z* 337.2383 (M+H)⁺; Δ + 0.4 mmu] data, which was fully supported by the ¹H and ¹³C NMR data. This formula indicated five degrees of unsaturation. The ¹H NMR and DEPT spectra in CD₃OD revealed the presence of five methyl groups, one olefinic methylene group (δ 112.1), four sp³ methylene groups, four sp² methines, and one oxygenated methine, requiring the presence of two hydroxyl groups. In addition to the signals corresponding to the above carbons, analysis of the ¹³C NMR spectrum revealed the presence of a ketone group (δ 203.1), one sp² quaternary carbon (δ 157.3), and three sp³ quaternary oxygenated carbons (δ 73.7, δ 74.7, and δ 84.2). Therefore, four of the five degrees of unsaturation required by the molecular formula were directly accounted by analysis of ¹³C NMR data, indicating the presence of an additional ring system in compound **1**. The planar structure of **1** was mainly elucidated on the basis of 2D-NMR data. Analysis of ¹H–¹H COSY and HMQC–TOCSY data disclosed proton–proton networks corresponding to the H1–H2, H4–H6, H8–H10, and H14–H16 (H17) substructures, along with isolated methylene (C-12) and methyl groups (C-18, C-19, and C-20). Long-range proton–carbon correlations observed in the HMBC spectrum of **1** provided corroborative evidences to support these subunits deduced from COSY and HMQC–TOCSY data. The presence of a disubstituted *E*-double bond at C5–C6 was implied by the *J* (H,H) value [H-5 (δ_H 5.65)/H-6 (δ_H 5.66): 15.8 Hz] obtained from the homonuclear decoupling experiment performed with irradiating signals for H₂–4. HMBC correlations of H₃–20 with C-2, C-3, and C-4 as well as of H-1 with C-3 revealed that the C1–C2 and C4–C6 subunits were joined at C-3. Similarly, HMBC correlations of H₃–19 with C-6, C-7, and C-8, along with correlations of H-5 with C-7 led to the extension of the carbon skeleton to C1–C10 with two quaternary carbons (C-3 and C-7) bearing methyl groups. Key HMBC correlations of the isolated

methylene unit H₂–12 with C-10, C-11, C-13, C-14, and C-18 allowed the completion of the carbon framework in the molecule. Correlations of H₃–18 with C-10, C-11, and C-12, and of H-14 with C-13 also supported this assignment. At this point, two hydroxyl groups and an oxygen atom remained to be accounted. Although chemical shifts considerations of C-3, C-7, C-10, and C-11 suggested that these carbons must be oxygenated, there was no positive evidence for assigning the positions of hydroxyl groups and ether ring closure. Therefore, complete gross structure of compound **1** was proposed on the basis of chemical shifts considerations and comparisons of the values with those of relevant carbons in the literatures. Inspection of ¹³C NMR chemical shifts in several natural products with structural features similar to those of **1** suggested that the oxygenated carbons in the dihydrofuran system resonated above 80 ppm, while the quaternary carbon bearing the hydroxyl group in the linear carbon skeleton usually resonated below 80 ppm.^{17–20} Thus, C-7 (δ 84.2) and C-10 (δ 85.7) were suggested to be connected via an oxygen atom to form a tetrahydrofuran ring system, and the remaining C-3 and C-11 were assigned to possess hydroxyl groups to complete the gross structure of **1** as shown. The relative configurations of the stereocenters at C-7 and C-10 were proposed on the basis of NOESY correlations of H-10 with H₃–18 and H₃–19, placing these protons on the same face of the ring system. However, the relative configurations at the C-3 and C-11 were not determined as it could not be related to those of the rest of the molecule.

HRESIMS spectrum [*m/z* 337.2374 (M+H)⁺; Δ – 0.5 mmu] for hueafuranoid B (**2**) indicated a molecular formula identical to that of **1**. The DEPT and ¹³C NMR data showed that the numbers of methyls, methylenes, methines, and quaternary carbons were identical to those of **1** (Tables 1 and 2). Furthermore, the ¹H and ¹³C NMR (Table 2) spectra were almost identical to those of **1**, except for the respective chemical shift differences for the positions at C-5, C-6, C-8, and C-9. This observation implied that compound **2** is a stereoisomer of hueafuranoid A (**1**), and detailed analysis of the 1D-, COSY, and HSQC NMR data revealed that **2** possessed the same planar structure as that of **1** (Table 2 and Supplementary data). The geometry of a disubstituted double bond at C5–C6 was assigned as *E* based on the *J* (H,H) value [H-5 (δ_H 5.62)/H-6 (δ_H 5.48): 15.7 Hz]. NOESY correlation of CH₃–18 with CH₃–19 suggested that these two methyl groups are placed on the same face

Table 1
NMR Data for hueafuranoid A (**1**) in CD₃OD

Position	δ_C^a	δ_H , mult ^b . (J in Hz)	HMBC (H → C#)
1	112.1	5.20, dd (17.6, 1.5) 5.02, dd (10.6, 1.5)	2, 3
2	146.3	5.92, dd (17.6, 10.6)	3
3	73.7	—	—
4	46.4	2.23, m	2, 3, 5, 6, 20
5	124.1	5.65, m	4, 6, 7
6	140.6	5.66, m	4, 5, 7
7	84.2	—	—
8	39.0	1.85, m 1.78, m	9
9	27.3	1.94, m 1.87, m	8, 10, 11
10	85.7	3.93, t, 7.0	12, 18
11	74.7	—	—
12	52.0	2.74, d (14.6) 2.47, d (14.6)	10, 11, 13, 14, 18
13	203.1	—	—
14	126.5	6.27, br s	13, 16, 17
15	157.3	—	—
16	20.9	2.13, d (1.1)	13, 14, 15, 17
17	27.8	1.91, d (1.1)	14, 15, 16
18	23.1	1.17, s	10, 11, 12
19	26.3	1.27, s	6, 7, 8
20	27.2	1.22, s	2, 3, 4

^a Recorded at 100 MHz.^b Recorded at 400 MHz.

of the tetrahydrofuran ring system. Therefore, the gross structure of **2** was assigned as shown.

HRESIMS data for hueafuranoid C (**3**) indicated that it has a molecular formula of C₂₀H₃₄O₄, which indicated that **3** has two more hydrogen atoms than **1** and **2**. The ¹H NMR data of **3** was similar to that of **1** except that two allylic methyl singlets (CH₃-16 and CH₃-17) observed in **1** were replaced by a pair of methyl doublets (δ 0.91), and that additional signals corresponding to one aliphatic methylene (δ 2.42) and one methine (δ 2.10) were appeared. The ¹³C NMR spectrum lacked two sp² carbons (δ 157.3 and δ 126.5) observed in the spectrum for **1**, but included additional resonances

for two sp³ carbons (δ 54.9 and δ 25.4). Taken together, it was suggested that the C14–C15 olefin group in **1** had been reduced in **3**. Analysis of the HSQC and COSY data confirmed this assignment (Supplementary data), and the chemical shifts for all elements in **3** were assigned by comparing them with the chemical shifts of **1**. The relative configuration of **3** was assigned by analysis of the NOESY data. NOESY correlation of H-10 with H₃-19 indicated that these protons are all on the same face of the ring system. Therefore, compound **3** was assigned to possess the same relative configuration of the tetrahydrofuran ring system as that of **1**.

The NMR data for hueafuranoid D (**4**), which has the identical molecular formula with that of **3**, were very similar to those of **3**. The primary difference in the ¹H NMR spectrum of **4** was that the signals for H-5 and H-6 were clearly distinctive as compared to those for **3** (Table 2). Careful examination of ¹H NMR spectra for compounds **1–3** revealed that compound **4** contains almost identical signals corresponding to the right side of the tetrahydrofuran ring system of compound **3**, while the portion of the ¹H NMR signals of **2** corresponding to the left side of the ring system is almost identical to the remaining portion of the ¹H NMR spectrum for **4**. These observations suggested that the structure of **4** is the reduced product of **2** at C-14–C15 olefin group, while it retains the same stereochemistry as that of **2**. This proposed structure for **4** was fully supported by analysis of the HSQC, COSY, and NOESY data (Table 2 and Supplementary data).

Hueafuranoid A (**1**) exhibited inhibitory effect against PTP1B activity in a dose-dependent manner with an IC₅₀ value of 13.9 μ M. The inhibitory activities of **2–4** could not be evaluated because of lack of materials. A known PTP1B inhibitor, ursolic acid (IC₅₀ = 3.08 μ M) was used as a positive control in the assay.^{21,22} Next, the kinetics of PTP1B inhibition by **1** were explored by using different concentrations of a substrate in an effort to elucidate the mode of inhibition. When *p*-nitrophenyl phosphate was used as a substrate, compound **1** decreased the *V*_{max} value, but did not alter the *K*_m value of PTP1B (Fig. 2). Therefore, it was shown that hueafuranoid A (**1**) behaves as a non-competitive inhibitor of PTP1B, implying that hueafuranoids may bind to the enzyme-substrate complex or to an allosteric site within PTP1B.²³

Table 2
¹H and ¹³C NMR Data for hueafuranoids B–D (**2–4**) in CD₃OD

position	2		3		4	
	δ_C^a	δ_H , mult ^b . (J in Hz)	δ_C^a	δ_H , mult ^b . (J in Hz)	δ_C^a	δ_H , mult ^b . (J in Hz)
1	112.1	5.17, dd (17.6, 1.5) 5.00, dd (11.0, 1.5)	112.1	5.17, dd (17.2, 1.5) 5.00, dd (10.6, 1.5)	112.1	5.17, dd (17.4, 1.6) 5.00, dd (10.8, 1.6)
2	146.2	5.90, dd (17.6, 11.0)	146.3	5.91, dd (17.2, 10.6)	146.2	5.91, dd (17.4, 10.8)
3	73.7	—	73.7	—	73.7	—
4	46.1	2.22, dd (7.0, 0.7)	46.4	2.22, m	46.3	2.22, dd (7.3, 1.0)
5	124.2	5.62, dt (15.7, 7.0)	124.1	5.63, m	124.2	5.62, dt (15.5, 7.3)
6	139.7	5.48, dt (15.7, 0.7)	140.6	5.64, m	139.7	5.48, dt (15.5, 1.0)
7	84.5	—	85.6	—	85.3	—
8	38.4	1.90, m 1.86, m	38.9	1.82, m 1.76, m	38.4	1.89, m 1.84, m
9	27.1	1.86, m 1.64, m	27.3	1.91, m 1.86, m	27.04	1.84, m 1.63, m
10	85.3	3.86, t (7.3)	84.2	3.92, t (6.6)	84.5	3.87, t (7.1)
11	74.8	—	74.3	—	74.3	—
12	52.1	2.72, d (14.3) 2.47, d (14.3)	51.1	2.75, d (14.6) 2.44, d (14.6)	51.2	2.73, d (14.8) 2.45, d (14.8)
13	203.2	—	213.7	—	213.7	—
14	126.5	6.27, m	54.9	2.42, m	54.8	2.43, dd (7.1, 3.3)
15	157.3	—	25.4	2.10, m	25.4	2.10, m
16	21.0	2.13, d (1.1)	23.0	0.91, d (6.6)	23.0	0.91, d (6.7)
17	27.8	1.91, d (1.1)	22.9	0.91, d (6.6)	22.9	0.91, d (6.7)
18	22.8	1.16, s	22.8	1.16, s	22.6	1.15, s
19	27.4	1.28, s	26.3	1.26, s	27.4	1.28, s
20	27.0	1.20, s	27.1	1.22, s	27.0	1.21, s

^a Recorded at 100 MHz.^b Recorded at 400 MHz.

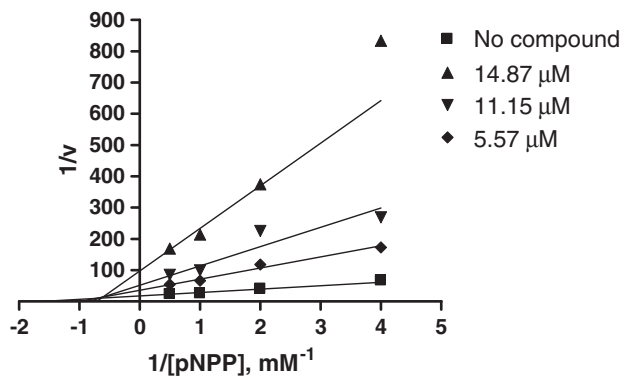


Figure 2. Kinetic analysis of PTP1B inhibition by hueafuranoid A (**1**) as illustrated by a Lineweaver–Burk plot. Data are expressed as mean initial velocity for $n = 3$ replicates at each substrate concentration. Concentrations (μM) of **1** are indicated in the figure.

To date, approximately over 1000 lichen metabolites have been identified so far, and most of them are a diverse array of phenolic compounds derived from polyketide biosynthetic pathway.^{10,11} In addition, lichens are known to produce terpenoids from the mevalonate pathway. Although triterpenes such as zeorin are fairly common among lichen metabolites, encountering diterpenes from lichens is quite rare. To the best of our knowledge, hueafuranoids are the first secondary metabolites reported from the genus *Huea*, and the discovery of these bioactive metabolites has further demonstrated that lichens from the Antarctic region could be important resources as new bioactive natural products.

Acknowledgment

This research was supported by a grant to the Korea Polar Research Institute (KOPRI) under a project PE12040.

Supplementary data

Supplementary data associated with this article can be found, in the online version, at <http://dx.doi.org/10.1016/j.bmcl.2012.10.063>.

References and notes

- Bialy, L.; Waldmann, H. *Angew. Chem., Int. Ed.* **2005**, *44*, 3814.
- Elchebly, M.; Payette, P.; Michaliszyn, E.; Cromlish, W.; Collins, S.; Loy, A. L.; Normandin, D.; Cheng, A.; Himms-Hagen, J.; Chan, C. C.; Ramachandran, C.; Gresser, M. J.; Tremblay, M. L.; Kennedy, B. P. *Science* **1999**, *283*, 1544.
- Koren, S.; Fantus, I. G. *Best Pract. Res. Clin. Endocrinol. Metab.* **2007**, *21*, 621.
- Klaman, L. D.; Boss, O.; Peroni, O. D.; Kim, J. K.; Martino, J. L.; Zabolotny, J. M.; Moghal, N.; Lubkin, M.; Kim, Y. B.; Sharpe, A. H.; Stricker-Krongrad, A.; Shulman, G. I.; Neel, B. G.; Kahn, B. B. *Mol. Cell. Biol.* **2000**, *20*, 5479.
- Zhang, S.; Zhang, Z.-Y. *Drug Discovery Today* **2007**, *12*, 373.
- Liu, S.; Zeng, L.-F.; Wu, L.; Yu, X.; Xue, T.; Gunawan, A. M.; Long, Y.-Q.; Zhang, Z.-Y. *J. Am. Chem. Soc.* **2008**, *130*, 17075.
- Zhang, Y.-N.; Zhang, W.; Hong, D.; Shi, L.; Shen, Q.; Li, J. Y.; Li, J.; Hu, L.-H. *Bioorg. Med. Chem. Lett.* **2008**, *16*, 8697.
- Huneck, S. *Naturwissenschaften* **1999**, *86*, 559.
- Ingólfssdóttir, K. *Phytochemistry* **2002**, *61*, 729.
- Wörgötter, E. S. *Nat. Prod. Rep.* **2008**, *25*, 188.
- Molnár, K.; Farkas, E. Z. *Naturforsch.* **2010**, *65*, 157.
- Kumar, K. C. S.; Müller, K. J. *Nat. Prod.* **1999**, *62*, 817.
- Seo, C.; Choi, Y. H.; Sohn, J. H.; Ahn, J. S.; Yim, J. H.; Lee, H. K.; Oh, H. *Bioorg. Med. Chem. Lett.* **2008**, *18*, 772.
- Seo, C.; Sohn, J. H.; Ahn, J. S.; Yim, J. H.; Lee, H. K.; Oh, H. *Bioorg. Med. Chem. Lett.* **2009**, *19*, 2801.
- Seo, C.; Choi, Y. H.; Ahn, J. S.; Yim, J. H.; Lee, H. K.; Oh, H. *J. Enzyme Inhib. Med. Chem.* **2009**, *24*, 1133.
- Seo, C.; Yim, J. H.; Lee, H. K.; Oh, H. *Mycology* **2011**, *2*, 18.
- Suzuki, M.; Matsuo, Y.; Takeda, S.; Suzuki, T. *Phytochemistry* **1993**, *33*, 651.
- Miller, S.; Tinto, W. F.; McLean, S.; Reynolds, W. F.; Yu, M.; Carter, C. A. G. *Tetrahedron* **1995**, *51*, 11959.
- Cueto, M.; Darias, J. *Tetrahedron* **1996**, *52*, 5899.
- Cueto, M.; Darias, J.; Roviro, J.; Martín, A. J. *Nat. Prod.* **1998**, *61*, 17.
- Na, M.; Tang, S.; He, L.; Oh, H.; Kim, B. S.; Oh, W. K.; Kim, B. Y.; Ahn, J. S. *Planta Med.* **2006**, *72*, 261.
- Zhang, W.; Hong, D.; Zhou, Y.; Zhang, Y.; Shen, Q.; Li, J.; Hu, L.; Li, J. *Biochem. Biophys. Acta* **2006**, *1760*, 1505.
- Wiesmann, C.; Barr, K. J.; Kung, J.; Zhu, J.; Erlanson, D. A.; Shen, W.; Fahr, B. J.; Zhong, M.; Taylor, L.; Randal, M.; McDowell, R. S.; Hansen, S. K. *Nat. Struct. Mol. Biol.* **2004**, *11*, 730.